Mathematical modeling quantifies ERK-activity in response to inhibition of the BRAFV600E-MEK-ERK cascade.

Sara Hamis,[1] Yury Kapelyukh,[2] Aileen McLaren,[2] Colin J. Henderson,[2] C. Roland Wolf,[2] Mark A.J. Chaplain.[1]

1 School of Mathematics and Statistics, University of St Andrews, St Andrews, Scotland, UK.
2 School of Medicine, Jacqui Wood Cancer Centre, Ninewells Hospital and Medical School, University of Dundee, Dundee, Scotland, UK.

Keywords: dabrafenib, trametinib, mitogen activated protein-kinase (MAPK), drug combination, Huang-Ferrell cascade model.

Financial support: All authors acknowledge support from the Medical Research Council [grant code MR/R017506/1].

Corresponding author name: Sara Hamis.

Corresponding author email address: sjh37@st-andrews.ac.uk.

Conflict of interest disclosure statement: The authors declare that they have no conflict of interest.

Pre-print posted in April 2021. This is version 1 of the pre-print article.

Abstract

Simultaneous inhibition of multiple components of the BRAF-MEK-ERK cascade (vertical inhibition) has become a standard of care for treating BRAF-mutant melanoma. However, the molecular mechanisms of how vertical inhibition synergistically suppress intracellular ERK activity, and as a consequence cell proliferation, are yet to be fully elucidated.

In this study, we develop a mechanistic mathematical model that describes how the mutant BRAF-inhibitor, dabrafenib, and the MEK-inhibitor, trametinib, affect signaling through the BRAFV600E-MEK-ERK cascade. We formulate a system of chemical reactions that describes cascade signaling dynamics and, using mass action kinetics, the chemical reactions are re-expressed as ordinary differential equations. Using model parameters obtained from *in vitro* data available in the literature, these equations are solved numerically to obtain the temporal evolution of the concentrations of the components in the signaling cascade.

Our mathematical model provides a quantitative method to compute how dabrafenib and trametinib can be used in combination to synergistically inhibit ERK activity in BRAFV600E mutant melanoma cells. This work elucidates molecular mechanisms of vertical inhibition of the BRAFV600E-MEK-ERK cascade and delineates how elevated cellular BRAF concentrations generate drug resistance to dabrafenib and trametinib. In addition, the computational simulations suggest that elevated ATP levels could be a factor in drug resistance to dabrafenib. The mathematical model that is developed in this study will have generic application in the improved design of anticancer combination therapies that target BRAF-MEK-ERK pathways.

Introduction

Mitogen-activated protein kinase (MAPK) pathways are present in all eukaryotic cells and play a pivotal role in cellular processes linked to proliferation, differentiation and apoptosis [1]. A general MAPK pathway consists of a three-tiered cascade, with a MAPK kinase kinase (MAPKKK) on the top tier, a MAPK kinase (MAPKK) on the middle tier, and a MAPK on the bottom tier. Via sequential kinase activation, signals can propagate through the MAPK cascade in which the activated MAPKKK phosphorylates, and thereby activates the MAPKK, which in turn phosphorylates, and thereby activates, the MAPK.

Several MAPKKK-MAPKK-MAPK cascades are present in eukaryotic cells, but in this study, we focus our attention on one such cascade: the BRAF-MEK-ERK cascade. Mutations in this signaling pathway have been identified as drivers for tumor development and growth, and therefore this cascade is of particular interest in the treatment of cancer.

Upon activation, ERK can phosphorylate numerous substrates in the cytoplasm and the nucleus and thereby regulate gene expression directly, by phosphorylating transcription factors such as Elk, Ets and Myc, and indirectly, by acting on substrates that in turn can modify transcription factors [2]. These phosphorylation events, which are controlled by both the amplitude and the duration of ERK activation, are crucial in regulating intracellular processes, including cell proliferation.

In the early 2000s, it was established that BRAF oncogene mutations occur in a majority of melanomas [3]. In melanomas harboring the BRAFV600E mutation, the most common BRAF mutation [4], the BRAF kinase is constitutively activated and thus signaling through the BRAF-MEK-ERK cascade is hyperactivated and always turned *on*, which can result in uncontrolled cell proliferation [5, 6]. As a consequence, small molecule inhibitors that target the BRAF-MEK-ERK cascade have been developed, with these inhibitors acting to inhibit the enzymatic activity of the kinases in the cascade [7]. Such inhibitors ultimately suppress the amount of activated ERK within a cell and, by extension, the cell's proliferative abilities. Such drugs have been shown to have profound anti-tumor effects.

Vertical inhibition describes a treatment approach in which two or more tiers in a cascade, such as the BRAF-MEK-ERK cascade, are concurrently targeted [8]. In this paper, we specifically investigate drug responses to mono- and combination therapies that include the BRAF-inhibitor dabrafenib and the MEK-inhibitor trametinib. Dabrafenib is an adenosine triphosphate (ATP)-competitive inhibitor with specificity for BRAFV600E, and trametinib is an allosteric inhibitor that selectively inhibits MEK1/2 [9].

In 2011, the first selective inhibitor of mutated BRAF, vemurafenib, was approved by the US Food and Drug Administration for treating BRAF-mutant metastatic or unresectable melanoma [10]. Thereafter, selective BRAF-inhibitors replaced the previously used chemotherapies in treating BRAFV600E and BRAFV600K mutant melanoma in clinics, which significantly improved patient survival [11]. However, drug resistance to BRAF-inhibiting monotherapies commonly develops within 6-8 months of treatment [12, 13, 14].

In current treatment protocols, combined BRAF and MEK inhibition is a standard of care for treating BRAFV600E mutant melanoma [12, 13, 15, 16]. Compared to BRAF inhibiting monotherapies, such combination therapies have been shown to delay the onset of drug resistance; in a clinical phase 3 trial, the median progression-free survival was respectively reported to be 5.8 and 9.4 months for dabrafenib mono-treatments and dabrafenib-trametinib combination treatments [13]. This, yet rapid, onset of drug resistance suggests that current treatment regimens create a pressure that selects for drug resistant tumor subclones [14].

Several mechanisms of drug resistance have been reported, one of which is BRAF gene amplification [4]. Xue *et al.* experimentally showed that, in order for BRAFV600E mutant sub-

clones to proliferate in a heterogeneous melanoma population, their intracellular BRAF-levels must surpass a certain concentration (or fitness threshold), with this threshold being dependent on the administered drug(s) and treatment schedule. If this fitness threshold is low, drug resistant, BRAF-amplified subclones will have a growth advantage, and consequently they will sweep the tumor and eventually render it drug resistant. However, if this fitness threshold is sufficiently high, subclones with amplified BRAF expression will have an evolutionary disadvantage to other subclones. As part of their study, Xue *et al.* showed, using patient derived xenografts, that an increased fitness threshold can be obtained via intermittent administration of vertical MAPK inhibition.

In order to further shed light on the effects of vertical inhibition of the BRAFV600E-MEK-ERK cascade at a molecular level, we here develop a mathematical model that mechanistically captures cascade dynamics in the presence of dabrafenib and trametinib. Huang & Ferrell developed the first mathematical model of a general MAPK pathway [17], consisting of a three-tiered cascade in which double phosphorylation of the MAPKKK, MAPKK and MAPK substrates is required for activation. Using mass action kinetics, Huang & Ferrell formulated the MAPK cascade in terms of a system of ordinary differential equations, which they solved numerically to simulate signaling dynamics within the cascade. Notably, the authors showed that the structure of the MAPK cascade yields ultra-sensitive signaling dynamics.

In this study, we modify Huang & Ferrell's model to capture cellular signaling dynamics in a specific MAPK pathway: the BRAF-MEK-ERK cascade in BRAFV600E mutant melanoma. As an extension to Huang & Ferrell's model, we introduce ATP-dependent substrate phosphorylation, and molecular drug actions of dabrafenib and trametinib.

Methods

We develop a mathematical model that simulates the temporal BRAF-MEK-ERK signaling dynamics in BRAFV600E mutant melanoma. In order to do this, we first map out the structure of the BRAF-MEK-ERK cascade, and identify the drug actions of dabrafenib and trametinib, that respectively inhibit enzymatic BRAF and MEK activity. From the cascade structure and drug actions, we formulate a system of chemical reactions which captures intracellular signaling dynamics. Using mass action kinetics, the system of chemical reactions is thereafter re-formulated as a system of ordinary differential equations (ODEs) which is solved numerically in order to simulate the temporal evolution of signaling molecule concentrations. A model output of particular importance is the concentration of activated ERK over time, as the ultimate goal of vertical inhibition of the BRAFV600E-MEK-ERK pathway is to suppress cells' activated ERK levels and, by extension, their proliferative abilities. All model parameters (*i.e.*, kinetic constants and total intracellular protein concentrations) are obtained from data available in the literature [17, 18, 19, 20, 21].

The BRAF-MEK-ERK cascade

We modify Huang & Ferrel's cascade model [17] to capture the signaling dynamics of the BRAF-MEK-ERK cascade in BRAFV600E mutant melanoma. Both cascades are respectively illustrated in Figures 1a and b. Here, and throughout this work, singly and doubly phosphorylated proteins are respectively denoted by the prefixes p and pp. Note that double phosphorylation is required for substrate activation, and that phosphatases (phosphs) dephosphorylate singly- and doubly phosphorylated MAPKK/MEK and MAPK/ERK. In our model, BRAF phosphorylates MEK and once MEK has been doubly phosphorylated, it in turn phosphorylates ERK, which becomes activated when doubly phosphorylated. As BRAF is constitutively activated in BRAFV600E-mutant melanoma [6], we have reduced the top tier

in our modified cascade to contain only activated BRAF. Since the model will include the drug actions of dabrafenib, which is an ATP-competitive inhibitor, and trametinib, which is an allosteric ATP inhibitor, we extend Huang & Ferrell's model to include ATP-dependent substrate phosphorylation. Thus, in our model, when a substrate and an ATP molecule bind to an enzyme (in the absence of drugs), the ATP molecule donates a phosphate group to the substrate, and the ATP converts to adenosine diphosphate (ADP) after the metabolic process.

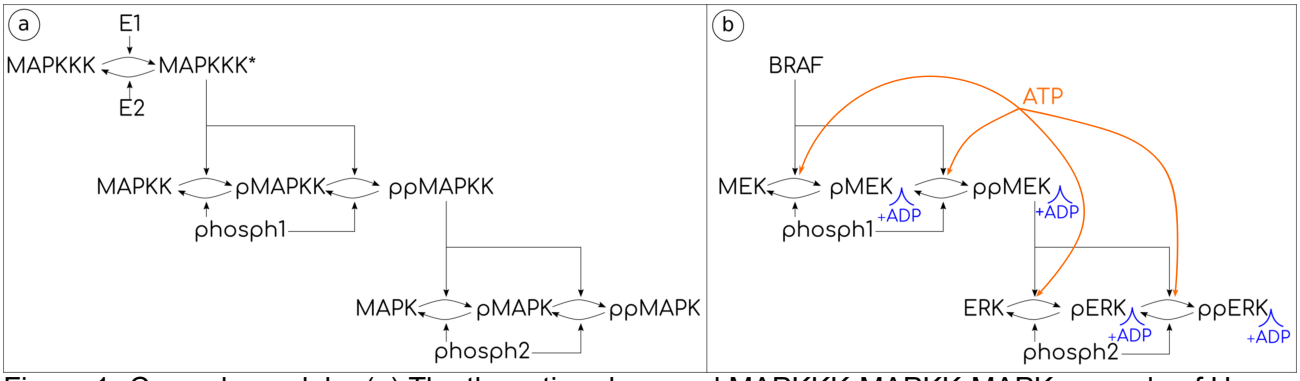

Figure 1: Cascade models. (a) The three-tiered general MAPKKK-MAPKK-MAPK cascade of Huang & Ferrell [17]. The star (*) denotes activated MAPKKK, and E1 and E2 are unspecified enzymes that respectively activate and inactivate MAPKKK. The prefixes p and pp denote singly and doubly phosphorylated proteins, and phosph1 and phosph2 are phosphatases that dephosphorylate MAPKK and MAPK respectively. (b) Our modified BRAF-MEK-ERK cascade in BRAFV600E mutant melanoma. BRAF is constitutively activated, and therefore the top cascade tier is reduced to a single node, activated BRAF. The modified cascade incorporates ATP-dependent substrate phosphorylation at the sites shown.

BRAF and MEK inhibitors

We model the pharmacodynamic actions of the two drugs dabrafenib and trametinib. Dabrafenib (DBF) is a potent and selective BRAF inhibitor, which is ATP-competitive [22]. As illustrated schematically in Figure 2 (top), DBF can thus bind to the ATP site of a BRAF molecule, and thereby inhibit BRAF-ATP reactions and the downstream phosphorylation of MEK and pMEK. Trametinib is classified as an allosteric MEK1/2 inhibitor, as it binds to a binding site that is distinct from, but adjacent to, the ATP binding site on the MEK molecule [23]. This is illustrated schematically in Figure 2 (bottom). MEK-bound trametinib prevents MEK from phosphorylating the substrates ERK and pERK.

The system of reactions

By combining the cascade illustrated in Figure 1b, with the drug actions that are schematically summarized in Figure 2, we formulate a system of chemical reactions that describes the signaling dynamics in the BRAFV600E-MEK-ERK cascade subjected to drugs. This results in a system of 36 chemical reactions (R.1-R.36), that are outlined in Figure 3, where the order of the binding events is considered.

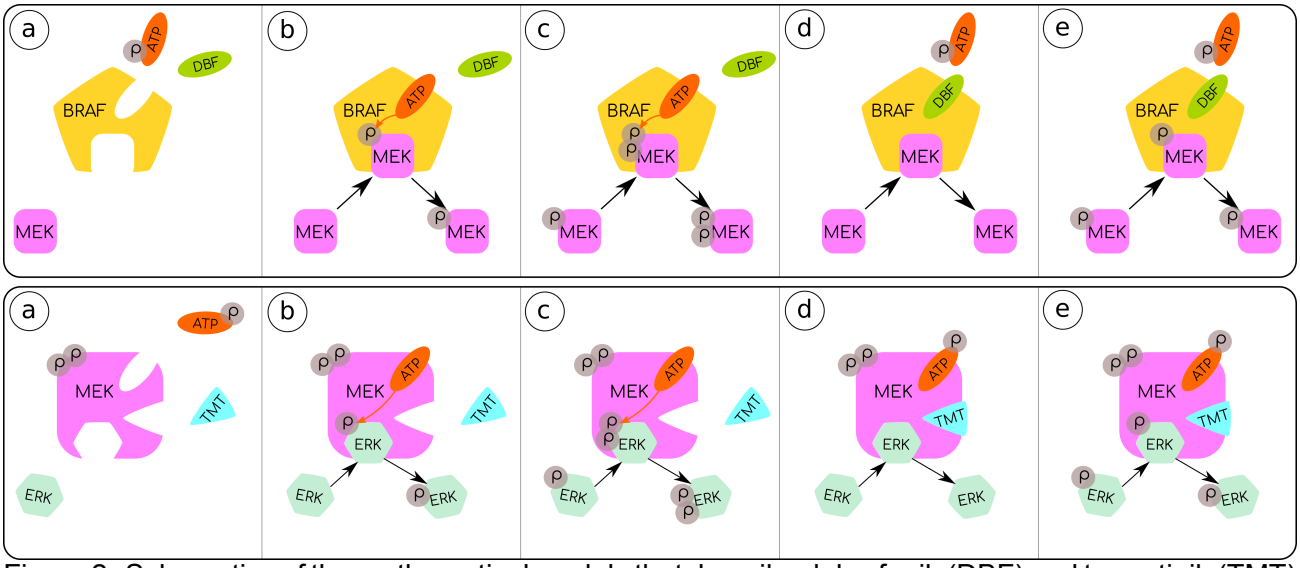

Figure 2: Schematics of the mathematical models that describe dabrafenib (DBF) and trametinib (TMT) drug actions. Top: (a) We consider two BRAF binding sites: one which can bind MEK and one which can bind ATP or dabrafenib. BRAF-bound ATP is necessary for the phosphorylation of MEK. (b) If ATP and MEK are bound to BRAF, then MEK is phosphorylated to the singly phosphorylated form pMEK. (c) If ATP and pMEK are bound to BRAF, then pMEK is phosphorylated to the doubly phosphorylated form ppMEK. (d) & (e) BRAF-bound dabrafenib prevents ATP from binding to BRAF, and thereby inhibits the phosphorylation of the substrates MEK and pMEK. Bottom: (a) We consider three MEK binding sites: one which can bind ERK, one which can bind ATP and one which can bind trametinib. ppMEK-bound ATP is necessary for the phosphorylation of ERK. (b) If ERK and ATP, but not TMT, are bound to ppMEK, then ERK is phosphorylated to the singly phosphorylated form pERK. (c) If pERK and ATP, but not TMT, are bound to ppMEK, then pERK is phosphorylated to the doubly phosphorylated form ppERK. (d) & (e) If TMT is bound to ppMEK, the phosphorylation of the substrates ERK and pERK is inhibited.

(R.1) $\text{BRAF} + \text{ATP} \underset{d_1}{\overset{a_1}{\rightleftharpoons}} \text{BRAF·ATP}$

(R.2) $\text{BRAF} + \text{MEK} \underset{d_2}{\overset{a_2}{\rightleftharpoons}} \text{BRAF·MEK}$

(R.3) $\text{BRAF} + \text{pMEK} \underset{d_2}{\overset{a_2}{\rightleftharpoons}} \text{BRAF·pMEK}$

(R.4) $\text{BRAF·ATP} + \text{MEK} \underset{d_2}{\overset{a_2}{\rightleftharpoons}} \text{BRAF·ATP·MEK} \xrightarrow{k_{12}} \text{BRAF} + \text{ADP} + \text{pMEK}$

(R.5) $\text{BRAF·ATP} + \text{pMEK} \underset{d_2}{\overset{a_2}{\rightleftharpoons}} \text{BRAF·ATP·pMEK} \xrightarrow{k_{12}} \text{BRAF} + \text{ADP} + \text{ppMEK}$

(R.6) $\text{BRAF·MEK} + \text{ATP} \underset{d_1}{\overset{a_1}{\rightleftharpoons}} \text{BRAF·ATP·MEK} \xrightarrow{k_{12}} \text{BRAF} + \text{ADP} + \text{pMEK}$

(R.7) $\text{BRAF·pMEK} + \text{ATP} \underset{d_1}{\overset{a_1}{\rightleftharpoons}} \text{BRAF·ATP·pMEK} \xrightarrow{k_{12}} \text{BRAF} + \text{ADP} + \text{ppMEK}$

(R.8) $\text{pMEK} + \text{phosph}_1 \underset{d_3}{\overset{a_3}{\rightleftharpoons}} \text{pMEK·phosph}_1 \xrightarrow{k_3} \text{MEK} + \text{phosph}_1$

(R.9) $\text{ppMEK} + \text{phosph}_1 \underset{d_3}{\overset{a_3}{\rightleftharpoons}} \text{ppMEK·phosph}_1 \xrightarrow{k_3} \text{pMEK} + \text{phosph}_1$

(R.10)* $\text{BRAF} + \text{DBF} \underset{d_4}{\overset{a_4}{\rightleftharpoons}} \text{BRAF·DBF}$

(R.11)* $\text{BRAF·MEK} + \text{DBF} \underset{d_4}{\overset{a_4}{\rightleftharpoons}} \text{BRAF·MEK·DBF}$

(R.12)* $\text{BRAF·pMEK} + \text{DBF} \underset{d_4}{\overset{a_4}{\rightleftharpoons}} \text{BRAF·pMEK·DBF}$

(R.13)* $\text{BRAF·DBF} + \text{MEK} \underset{d_2}{\overset{a_2}{\rightleftharpoons}} \text{BRAF·MEK·DBF}$

(R.14)* $\text{BRAF·DBF} + \text{pMEK} \underset{d_2}{\overset{a_2}{\rightleftharpoons}} \text{BRAF·pMEK·DBF}$

(R.15) $\text{ppMEK} + \text{ATP} \underset{d_5}{\overset{a_5}{\rightleftharpoons}} \text{ppMEK·ATP}$

(R.16) $\text{ppMEK} + \text{ERK} \underset{d_6}{\overset{a_6}{\rightleftharpoons}} \text{ppMEK·ERK}$

(R.17) $\text{ppMEK} + \text{pERK} \underset{d_6}{\overset{a_6}{\rightleftharpoons}} \text{ppMEK·pERK}$

(R.18) $\text{ppMEK·ATP} + \text{ERK} \underset{d_6}{\overset{a_6}{\rightleftharpoons}} \text{ppMEK·ATP·ERK} \xrightarrow{k_{56}} \text{ppMEK} + \text{ADP} + \text{pERK}$

(R.19) $\text{ppMEK·ATP} + \text{pERK} \underset{d_6}{\overset{a_6}{\rightleftharpoons}} \text{ppMEK·ATP·pERK} \xrightarrow{k_{56}} \text{ppMEK} + \text{ADP} + \text{ppERK}$

(R.20) $\text{ppMEK·ERK} + \text{ATP} \underset{d_5}{\overset{a_5}{\rightleftharpoons}} \text{ppMEK·ATP·ERK} \xrightarrow{k_{56}} \text{ppMEK} + \text{ADP} + \text{ppERK}$

(R.21) $\text{ppMEK·pERK} + \text{ATP} \underset{d_5}{\overset{a_5}{\rightleftharpoons}} \text{ppMEK·ATP·pERK} \xrightarrow{k_{56}} \text{ppMEK} + \text{ADP} + \text{ppERK}$

(R.22) $\text{pERK} + \text{phosph}_2 \underset{d_7}{\overset{a_7}{\rightleftharpoons}} \text{pERK·phosph}_2 \xrightarrow{k_7} \text{ERK} + \text{phosph}_2$

(R.23) $\text{ppERK} + \text{phosph}_2 \underset{d_7}{\overset{a_7}{\rightleftharpoons}} \text{ppERK·phosph}_2 \xrightarrow{k_7} \text{pERK} + \text{phosph}_2$

(R.24)** $\text{ppMEK} + \text{TMT} \underset{d_8}{\overset{a_8}{\rightleftharpoons}} \text{ppMEK·TMT}$

(R.25)** $\text{ppMEK·ATP} + \text{TMT} \underset{d_8}{\overset{a_8}{\rightleftharpoons}} \text{ppMEK·ATP·TMT}$

(R.26)** $\text{ppMEK·ERK} + \text{TMT} \underset{d_8}{\overset{a_8}{\rightleftharpoons}} \text{ppMEK·ERK·TMT}$

(R.27)** $\text{ppMEK·pERK} + \text{TMT} \underset{d_8}{\overset{a_8}{\rightleftharpoons}} \text{ppMEK·pERK·TMT}$

(R.28)** $\text{ppMEK·ERK·ATP} + \text{TMT} \underset{d_8}{\overset{a_8}{\rightleftharpoons}} \text{ppMEK·ERK·ATP·TMT}$

(R.29)** $\text{ppMEK·pERK·ATP} + \text{TMT} \underset{d_8}{\overset{a_8}{\rightleftharpoons}} \text{ppMEK·pERK·ATP·TMT}$

(R.30)** $\text{ppMEK·TMT} + \text{ATP} \underset{d_5}{\overset{a_5}{\rightleftharpoons}} \text{ppMEK·ATP·TMT}$

(R.31)** $\text{ppMEK·TMT} + \text{ERK} \underset{d_6}{\overset{a_6}{\rightleftharpoons}} \text{ppMEK·ERK·TMT}$

(R.32)** $\text{ppMEK·TMT} + \text{pERK} \underset{d_6}{\overset{a_6}{\rightleftharpoons}} \text{ppMEK·pERK·TMT}$

(R.33)** $\text{ppMEK·TMT·ERK} + \text{ATP} \underset{d_5}{\overset{a_5}{\rightleftharpoons}} \text{ppMEK·ERK·ATP·TMT}$

(R.34)** $\text{ppMEK·TMT·pERK} + \text{ATP} \underset{d_5}{\overset{a_5}{\rightleftharpoons}} \text{ppMEK·pERK·ATP·TMT}$

(R.35)** $\text{ppMEK·TMT·ATP} + \text{ERK} \underset{d_6}{\overset{a_6}{\rightleftharpoons}} \text{ppMEK·ERK·ATP·TMT}$

(R.36)** $\text{ppMEK·TMT·ATP} + \text{pERK} \underset{d_6}{\overset{a_6}{\rightleftharpoons}} \text{ppMEK·pERK·ATP·TMT}$

Figure 3: System of reactions (R.1-R.36) describing the signaling dynamics in the BRAFV600E-MEK-ERK cascade subjected to the drugs dabrafenib (DBF) and trametinib (TMT). The dot-notation (·) denotes complexes of two or more molecules. Reactions involving dabrafenib and trametinib are respectively marked by single (*) and double (**) stars.

The system of ordinary differential equations

We use the law of mass action to re-express the system of reactions (R.1-R.36) as a system of ODEs. In the system of ODEs, the dependent variables are the concentrations of the signaling molecules that occur in (R.1-R.36), and the independent variable is time. In short, the law of mass action says that the rate of a chemical reaction is proportional to the product of the masses of the reactants. Thus, the first reaction, R.1, which includes the molecules BRAF, ATP and BRAF·ATP, yields the following contributions to the system of ODEs,

$$\frac{d[BRAF]}{dt} = -a1[BRAF][ATP] + d1[BRAF \cdot ATP], \tag{1a}$$

$$\frac{d[ATP]}{dt} = -a1[BRAF][ATP] + d1[BRAF \cdot ATP], \tag{1b}$$

$$\frac{d[BRAF \cdot ATP]}{dt} = +a1[BRAF][ATP] - d1[BRAF \cdot ATP], \tag{1c}$$

where concentrations are denoted by square brackets surrounding the signaling molecule of interest, and t denotes time. Note that the right-hand sides of Equations 1a-c are subsequently extended to include more equations derived from other reactions in the system of reactions outlined in Figure 3. The full system of ODEs (O.1-O.36), is available in the Supplementary Material (SM1). In this work, we combine (O.1-O.36) with a set of system conservation laws (C.1-C.7 in SM1) to formulate a system of differential algebraic equations that we solve numerically to obtain the temporal evolution of the system molecule concentrations.

Model implementation

We implement and solve the system of ODEs (O.1-O.36), with conservation laws (C.1-C.7) *in silico*, in order to simulate the signaling dynamics in the BRAF-MEK-ERK cascade. The *in silico* model, which is developed using the programing language and computing environment MATLAB, is available on the code hosting platform GitHub. Instructions on how to access, run and modify the program are available in the Supplementary Material (SM2).

Model parameters

The system of reactions (R.1-R.36) includes eight forward rate constants $a_1, a_2, ..., a_8$, eight reverse rate constants $d_1, d_2, ..., d_8$ and four catalytic rate constants $k_{1,2}, k_3, k_{5,6}, k_7$. The values of these constants are listed in Table 1. Huang & Ferrell [17] argued that, when computing steady-state enzyme levels, it is not the individual rate constants, but rather the Michaelis constants, $K_{mi} = (d_i + k_i)/a_i$, that are important. We therefore set all forward rate constants a_i to be the same so that $a_j = a_1$ for all $j = 2, 3, .., 8$. We then use data available in the literature to set the parameter values for a_1, the eight reverse rate constants and the four catalytic rate constants, as is outlined in the Supplementary Material (SM3). The model initial condition, *i.e.*, a vector that includes the molecule concentrations at the start of the simulation, is also obtained from data in the literature [17, 19]. Initial molecule concentrations are listed in Table 2.

Rate constants in the system of reactions (R.1-R.36)				
constant	value	reference	description	appearance
a_1	0.106μM^{-1}s^{-1}	[17, 18]	Forward rate constant for ATP binding to BRAF (or a BRAF complex with MEK/pMEK).	R.1,R.6,R.7
d_1	6.23 s^{-1}	[17, 18, 24]	Reverse rate constant for ATP binding to BRAF (or a BRAF complex with MEK/pMEK).	R.1,R.6,R.7
a_2	0.106μM^{-1}s^{-1}	†	Forward rate constant for MEK/pMEK binding to BRAF (or a BRAF complex with ATP/DBF).	R.2,R.3,R.4, R.5,R.13,R.14
d_2	0.02385 s^{-1}	[17, 18]	Reverse rate constant for MEK/pMEK binding to BRAF (or a BRAF complex with ATP/DBF).	R.2,R.3,R.4, R.5,R.13,R.14
$k_{1,2}$	0.66 s^{-1}	[18]	Catalytic rate constant for production of pMEK/ppMEK from BRAF·ATP complex with MEK/pMEK.	R.4,R.5,R.6, R.7
a_3	0.106μM^{-1}s^{-1}	†	Forward rate constant for phosph$_1$ binding to pMEK/ppMEK.	R.8,R.9
d_3	0.0159 s^{-1}	[17, 18]	Reverse rate constant for phosph$_1$ binding to pMEK/ppMEK.	R.8,R.9
k_3	0.0159 s^{-1}	[17, 18]	Catalytic rate constant for production of MEK/pMEK from phosph$_1$ complex with pMEK/ppMEK.	R.8,R.9
a_4	0.106μM^{-1}s^{-1}	†	Forward rate constant for the drug DBF binding to BRAF (or a BRAF complex with MEK/pMEK).	R.10,R.11,R.12
d_4	0.0000593 s^{-1}	[17, 18, 20, 25, 26, 27]	Reverse rate constant for the drug DBF binding to BRAF (or a BRAF complex with MEK/pMEK).	R.10,R.11,R.12
a_5	0.106μM^{-1}s^{-1}	†	Forward rate constant for ATP binding to ppMEK (or a ppMEK complex with ERK/pERK/TMT/TMT&ERK/TMT&pERK).	R.15,R.20,R.21, R.30,R.33,R.34
d_5	0.3468 s^{-1}	[17, 18, 19]	Reverse rate constant for ATP binding to ppMEK (or a ppMEK complex with ERK/pERK/TMT/TMT&ERK/TMT&pERK).	R.15,R.20,R.21, R.30,R.33,R.34
a_6	0.106μM^{-1}s^{-1}	†	Forward rate constant for ERK/pERK binding to ppMEK (or a ppMEK complex with ATP/TMT/TMT&ATP).	R.16,R.17,R.18, R.19,R.31,R.32, R.35,R.36
d_6	0.01184 s^{-1}	[17, 18, 19]	Reverse rate constant for ERK/pERK binding to ppMEK (or a ppMEK complex with ATP/TMT/TMT&ATP).	R.16,R.17,R.18, R.19,R.31,R.32, R.35,R.36
$k_{5,6}$	0.0242 s^{-1}	[19]	Catalytic rate constant for production of pERK/ppERK from ppMEK·ATP complex with ERK/pERK.	R.18,R.19,R.20, R.21
a_7	0.106μM^{-1}s^{-1}	†	Forward rate constant for phosph$_2$ binding to pERK/ppERK.	R.22,R.23
d_7	0.0159 s^{-1}	[17, 18]	Reverse rate constant for phosph$_2$ binding to pERK/ppERK.	R.22,R.23
k_7	0.0159 s^{-1}	[17, 18]	Catalytic rate constant for production of ERK/pERK from phosph$_2$ complex with pERK/ppERK.	R.22,R.23
a_8	0.106μM^{-1}s^{-1}	†	Forward rate constant for the drug TMT binding to ppMEK (or a ppMEK complex with ATP/ERK/pERK/ERK&ATP/pERK&ATP).	R.24,R.25,R.26, R.27,R.28,R.29
d_8	0.0012296 s^{-1}	[17, 18, 21]	Reverse rate constant for the drug TMT binding to ppMEK (or a ppMEK complex with ATP/ERK/pERK/ERK&ATP/pERK&ATP).	R.24,R.25,R.26, R.27,R.28,R.29

Table 1: A table of the rate constants appearing in the system of reactions (R.1-R.36). The system includes eight forward rate constants $a_1, a_2, .., a_8$, eight reverse rate constants $d_1, d_2, .., d_8$, and four catalytic rate constants $k_{1,2}, k_3, k_{5,6}, k_7$. Stroke symbols (/) in the description column denote 'or', whilst ampersand symbols (&) denote 'and'. The rightmost column describes in which of the reactions (R.1-R.36) the constants appear. † All forward rate constants are of the same value.

Initial concentrations		
Initial condition	value	reference
[BRAF](0)	3-10 nM*	[17]
[MEK](0)	1.2 μM	[17]
[ERK](0)	1.2 μM	[17]
[phosph1](0)	0.3 nM	[17]
[phosph2](0)	0.12 μM	[17]
[ATP](0)	1-5 mM**	[19]
[DBF](0)	*applied DBF dose* (here 0-10 μM)	
[TMT](0)	*applied TMT dose* (here 0-10 μM)	

Table 2: Initial model concentrations, where the (0) notation denotes 'at time zero'. For molecule concentrations not listed in this table, the initial conditions is 0 μM. *Huang & Ferrell [17] listed MAP-KKK=3nM, and we use this as our baseline value. However, in order to study amplified BRAF levels as a mode of drug resistance, we explore initial BRAF concentrations within the range 3-10 nM. Similarly, initial ATP concentrations are explored within the range 1-5mM, but the baseline value is 1mM.

Results

Using the *in silico* model that we have developed, the temporal evolution of the concentration of all signaling components appearing in the system of reactions (R.1-R.36) are computed. In this study, our main model output of interest is activated ERK. For ease of presentation, we define a measure activated ERK, as a time-dependent fraction,

$$\text{activated ERK } = \frac{[ppERK](t)}{ERK_{tot}}, \tag{2}$$

where ERK_{tot} denotes the total amount of ERK in the system, such that ERK_{tot}= [ERK](0), as listed in Table 2.

Monotherapy results

We initially investigate how activated ERK levels within a cell vary in response to dabrafenib or trametinib monotherapy. The temporal evolution of activated ERK in response to these monotherapies are shown in Figures 4a and b respectively. Activated ERK levels at specific time points are plotted over intracellular concentrations of BRAF (left panel) and ATP (right panel) for different doses of dabrafenib (Figure 1c) and trametinib (Figure 1d).

The simulation data show that the modelled dabrafenib treatment responses are highly dynamic in time, and dependent on both intracellular BRAF and ATP concentrations (Figures 1a and 1c). These data also suggest that increased concentrations of BRAF and ATP make the cells less sensitive to dabrafenib. Further, these data show that the activated ERK levels eventually reach the same steady state value for several dabrafenib-BRAF-ATP concentration combinations (see also Supplementary Material, SM4).

In order for a cell to progress from the G1 to the S phase of the cell cycle, sustained ERK activity throughout the G1 phase is required, where ERK downregulates several anti-proliferative genes until S phase entry [28, 29]. This suggests that, if ERK activity can be suppressed for the duration of the G1 cell cycle phase, further cell cycle progression, and thus cell proliferation, can be inhibited.

In response to different trametinib doses, activated ERK levels reach distinct steady-state levels (Figure 1b). Moreover, trametinib treatment responses at time points after 8 hours are only sensitive to BRAF variations for low BRAF concentrations (under 3nM) and the efficacy of trametinib treatments is not sensitive to variations in ATP within the range of concentrations tested (Figure 1d).

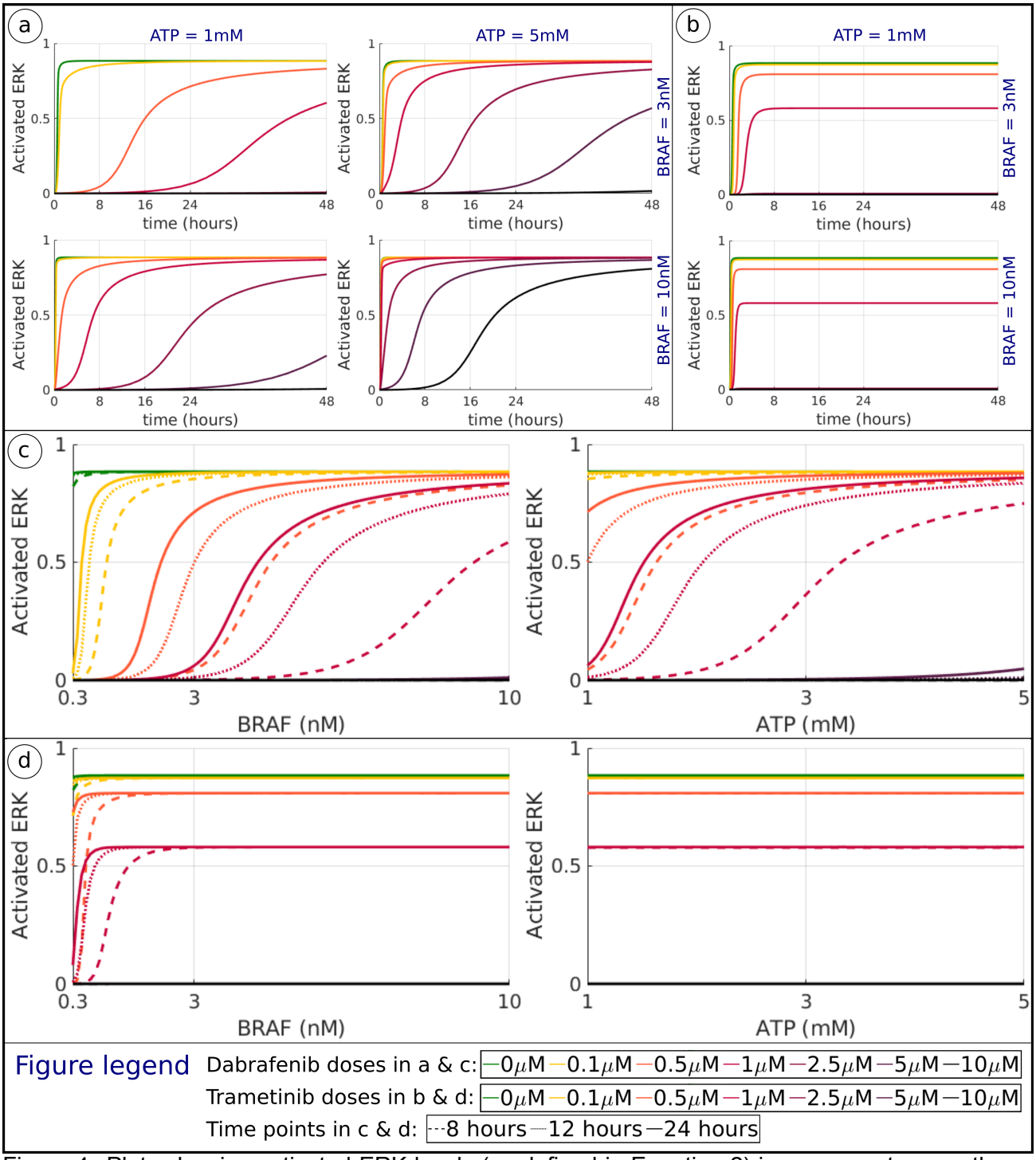

Figure 4: Plots showing activated ERK levels (as defined in Equation 2) in response to monotherapies of dabrafenib or trametinib. (a) The temporal evolution of activated ERK. Results are shown for different intracellular concentrations of BRAF, ATP and dabrafenib (DBF). (b) The temporal evolution of activated ERK. Results are shown for different intracellular concentrations of BRAF and trametinib (TMT). (c,d) Activated ERK levels are plotted over intercellular BRAF concentrations, where ATP concentrations are fixed at the baseline value 1mM (left). Activated ERK levels plotted over intercellular ATP concentrations, where BRAF concentrations are fixed at the baseline value 3nM (right). Results at 8, 16, and 24 hours are shown in dashed, dotted and solid lines respectively for different doses of dabrafenib (c) and trametinib (d).

Combination therapy results

We next evaluate the effect of combination therapies involving dabrafenib and trametinib on treatment outcome (Figure 5). When dabrafenib concentrations are zero (*i.e.*, for trametinib monotherapies) the activated ERK levels do not vary between 8 to 24 hours. However, when trametinib concentrations are zero (*i.e.*, for dabrafenib monotherapies) the activated ERK levels do vary between 8 to 24 hours and, as a consequence, so does dabrafenib-trametinib combination therapies (Figure 5a-c).

In order to determine whether there is dabrafenib-trametinib synergism we included an isobole that connects the two monotherapy doses that yield an activated ERK level of 0.5 (Figure 5a). Since drug combinations below this line can achieve activated ERK levels lower than 0.5, the drug combination is categorized as synergistic [30]. In Figures 5b and c, the BRAF and ATP levels have been increased from the baseline parameter values. By comparing Figure 5a, with Figures 5b and c, we can see that activated ERK levels increase with increased BRAF and ATP levels. Our mathematical model therefore predicts that increased intracellular BRAF and ATP concentrations will generate resistance to dabrafenib-trametinib combination therapies.

The influence of BRAF concentration on dabrafenib-trametinib efficacy is also reflected in Figure 5d. We see from these results the minimum BRAF concentration that is required to achieve an activated ERK level of 0.5 at 24 hours (when ATP is fixed at the baseline value 1 mM). Similarly, the minimum ATP concentration that is required to achieve an activated ERK level of 0.5 at 24 hours (when BRAF is fixed at the baseline value 3 nM) is visualized in Figure 5e.

Discussion

Although targeted anticancer drugs can generate patient responses in tumors previously intractable to treatment, there remain major issues in their clinical use. In particular, tumor regrowth due to rapid onset of drug resistance. A number of mechanisms of drug resistance have been described for example for drugs targeted at mutant BRAF in the MAPK pathway. Many of these involve the modulation of components of the pathway *e.g.*, by mutation or gene amplification. This results in the sustained activation of ERK in the presence of drug. As a consequence, drugs targeted at multiple components of the same pathway have been used in combination *e.g.*, BRAF and MEK inhibitors. Although this has resulted in some patient benefit, this has not resolved the problem and major challenges still remain. There is currently great interest in further developing the complexity of combination treatments. In the case of the BRAF pathway, for example, by the addition of an inhibitor of ERK [4].

Increasing treatment complexity however raises some major pharmacological challenges, including which drugs to use in combination and what doses to use in order to keep toxicity at an acceptable level. The vast number of drug combinations and dosing regimens which could be evaluated make it impossible to test all these either in the laboratory or in the clinic. Informative *in silico* pharmacological models are therefore needed.

Several research groups have analyzed and modified Huang & Ferrell's MAPK cascade model since it was presented in 1996 [17], as is summarized in a review by Orton *et al.* [2]. Mathematical analysis and computational simulation of the MAPK cascade model has explained how the dual phosphorylation and dephosphorylation events mechanistically give rise to the ultrasensitivity of ERK activation [31, 32] and bistability [33]. Integrated *in vitro*-mathematical work has further demonstrated switch-like (on or off) ERK activity in single cells in Xenopus oocytes subjected to progesterone [34]. Moreover, MAPK cascade models of various complexities have been presented and investigated in the literature, where these have

included *e.g.*, the internalization and downstream signaling activity of the epidermal growth factor receptor [35, 36].

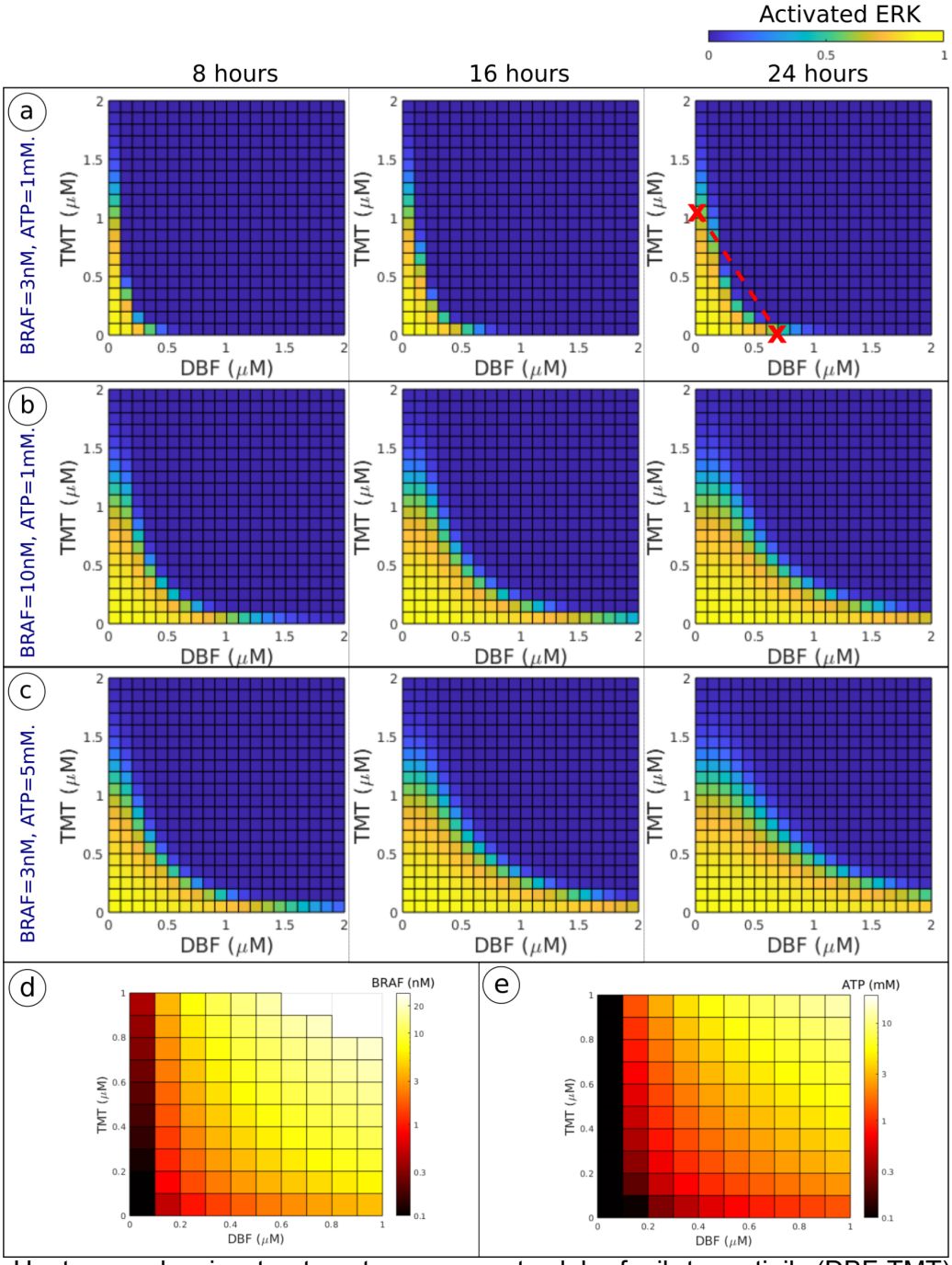

Figure 5: Heatmaps showing treatment responses to dabrafenib-trametinib (DBF-TMT) combination therapies. For each square in the heatmap, the horizontal axis of the intersection denotes the dabrafenib dose, and the vertical axis denotes the trametinib dose. (a,b,c) The fraction of activated ERK (as defined in Equation 2) at 8, 16 and 24 hours are shown in the left, middle and right columns respectively. BRAF and ATP concentrations vary between (a), (b) and (c). The right panel in (a) includes an isobole that connects the two monotherapy drug doses that yield an activated ERK level of 0.5 with a straight red line. Drug combinations below this line that yield activated ERK levels of 0.5 or less are categorized as synergistic. (d,e) The minimum BRAF (d) and ATP (e) concentrations that are required to yield an activated ERK level over 0.5, at 24 hours are shown. In (d), the ATP concentration is fixed at 1 mM. In (e), the BRAF concentration is fixed at 3 nM. For DBF-TMT combination doses where the activated ERK does not surpass 0.5 for BRAF concentrations under 20 nM, the squares in the heatmap in (d) are not colored.

To our knowledge, the mathematical model presented in this paper is the first MAPK cascade model to (i) specifically capture signaling dynamics in the BRAFV600E-MEK-ERK cascade, (ii) explicitly include ATP-dependent substrate phosphorylation, and (iii) include mechanistic drug actions of dabrafenib and trametinib, where the model parameters involved in $(i - iii)$ are obtained from published *in vitro* data.

In this paper, we have developed a mathematical model that captures signaling dynamics in the BRAFV600E-MEK-ERK cascade, in response to dabrafenib and trametinib treatments. Our *in silico* model can be used to quantify the temporal evolution of system molecule concentrations and, as a consequence, ERK activity. The model predicts that increased cellular BRAF and ATP concentrations will result in reduced sensitivity to dabrafenib-trametinib combination therapies. The prediction that ATP levels may be a factor introduces an important variable to take into consideration and suggests that the ATP level within a heterogeneous tumor cell population is a further factor in defining the outcome of treatment. Our finding is also consistent with experimental data showing that increased BRAF concentration is associated with drug resistance [4]. Whilst simulation of the ERK activation level at different concentrations of dabrafenib and 3 nM BRAF closely followed that observed in patients[37], an increase of the BRAF level to 10 nM in our model, similar to that found in drug resistant patient derived xenografts [4], predicted marked resistance of the ERK activation to treatment with dabrafenib (Figure 6).

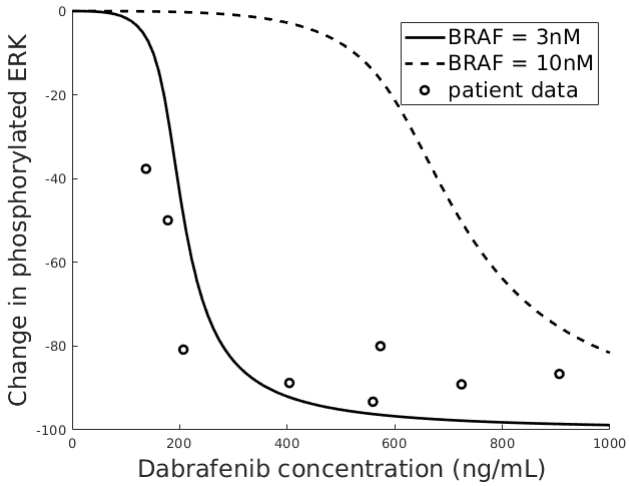

Figure 6: Plots showing changes is phosphorylated ERK ([pERK]+[ppERK]) from the baseline (no drug) level. Simulation results at 8 hours, when the ATP concentration is fixed at 1mM, are shown for BRAF concentrations of 3 and 10nM. The circles show patient data from a clinical study by Falchook *et al.* [37].

In order to investigate three-drug vertical inhibition of the BRAF-MEK-ERK pathway in BRAF-V600E mutant melanoma, the model could directly be extended to include the effects of an ERK inhibitor. As a further development of the modeling, one could study the effects of dabrafenib-trametinib treatment scheduling in a multi-cellular system using a multi-scale, agent-based model (ABM) [38, 39]. In order to implement the pathway model into an ABM, the relationship between ERK activity and cell cycle progression/inhibition and cell death needs to be established [28, 29, 40]. This is one aim of our future modelling studies. ABMs are naturally able to incorporate spatio-temporal variations in intracellular BRAF and ATP concentrations amongst cells, where these variations are derived from both genetic, phenotypic and environmental factors [41, 42]. ABMs can thus be used to simulate how drug resistant tumor subclones (*e.g.*, melanoma cells with elevated BRAF-levels) and drug sensitive tumor

subclones evolve in time and space in response to various drug combinations, drug doses and drug treatment schedules.

Thus, via a data-driven and bottom-up modelling approach [43], the *in silico* model developed in this study can be built upon to simulate how BRAF-MEK-ERK inhibition affects, not only intracellular ERK activity, but also, the progression of drug resistance in melanoma tumors. Previous experimental work has shown that drug combinations, drug doses, and treatment schedules all impact the evolution of drug resistant tumor subclones in melanoma, when the tumors are subjected to inhibitors that target the BRAF-MEK-ERK pathway [4, 44].

The predictive power of quantitative *in silico* models, such as that described here, are dependent on the accuracy of the kinetic constants for the different components of the signaling cascade as well as on the relative concentrations of the individual enzymes in the cascade. We would suggest that in the light of their key importance further studies are needed to validate the accuracy of the kinetic constants used. Indeed, translating such models to the treatment of individual cancer patients in the future may require the concentration and activity of the signaling components to be measured on an individual basis.

The mathematical model described in this study provides a method to quantitatively assess how vertical dabrafenib-trametinib inhibition suppresses ERK activity. We note that the modelling approach outlined in this paper can also be applied to other signaling cascades targeted in cancer treatment. Mathematical oncology models that are developed alongside experiments can be used to systematically motivate which drug combinations, drug doses and treatment schedules warrant experimental investigation [39].

References

[1] M. Cargnello and P. P. Roux. “Activation and function of the MAPKs and their substrates, the MAPK-activated protein kinases”, *Microbiol Mol Biol Rev* 75.1 (2011), pp. 50–83.

[2] R. J. Orton, O. E. Sturm, V. Vyshemirsky, M. Calder, D. R. Gilbert, and W. Kolch. “Computational modelling of the receptor-tyrosine-kinase-activated MAPK pathway”, *Biochem J* 392.Pt 2 (2005), pp. 249–261.

[3] H. Davies, G. R. Bignell, C. Cox, P. Stephens, S. Edkins, S. Clegg, et al. “Mutations of the BRAF gene in human cancer”, *Nature* 417.6892 (2002), pp. 949–954.

[4] Y. Xue, L. Martelotto, T. Baslan, A. Vides, M. Solomon, T. T. Mai, et al. “An approach to suppress the evolution of resistance in BRAFV600E-mutant cancer”, *Nat Med* 23.8 (2017), pp. 929–937.

[5] M. Karasarides, A. Chiloeches, R. Hayward, D. Niculescu-Duvaz, I. Scanlon, F. Friedlos, et al. “B-RAF is a therapeutic target in melanoma”, *Oncogene* 23.37 (2004), pp. 6292–6298.

[6] S. McGettigan. “Dabrafenib: A New Therapy for Use in BRAF-Mutated Metastatic Melanoma”, *J Adv Pract Oncol* 5.3 (2014), pp. 211–215.

[7] U. Degirmenci, M. Wang, and J. Hu. “Targeting Aberrant RAS/RAF/MEK/ERK Signaling for Cancer Therapy”, *Cells* 9.1 (2020).

[8] I. Ozkan-Dagliyan, J. N. Diehl, S. D. George, A. Schaefer, B. Papke, K. Klotz-Noack, et al. “Low-Dose Vertical Inhibition of the RAF-MEK-ERK Cascade Causes Apoptotic Death of KRAS Mutant Cancers”, *Cell Rep* 31.11 (2020), p. 107764.

[9] J. J. Luke and F. S. Hodi. “Ipilimumab, vemurafenib, dabrafenib, and trametinib: synergistic competitors in the clinical management of BRAF mutant malignant melanoma”, *Oncologist* 18.6 (2013), pp. 717–725.

[10] L. Shelledy and D. Roman. “Vemurafenib: First-in-Class BRAF-Mutated Inhibitor for the Treatment of Unresectable or Metastatic Melanoma.”, *J Adv Pract Oncol.* 6.4 (2015), pp. 361–365.

[11] E. T. Tanda, I. Vanni, A. Boutros, V. Andreotti, W. Bruno, P. Ghiorzo, et al. “Current State of Target Treatment in BRAF Mutated Melanoma”, *Front Mol Biosci* 7 (2020), p. 154.

[12] C. Robert, B. Karaszewska, J. Schachter, P. Rutkowski, A. Mackiewicz, D. Stroiakovski, et al. “Improved overall survival in melanoma with combined dabrafenib and trametinib”, *N Engl J Med* 372.1 (2015), pp. 30–39.

[13] G. V. Long, D. Stroyakovskiy, H. Gogas, E. Levchenko, F. de Braud, J. Larkin, et al. “Combined BRAF and MEK inhibition versus BRAF inhibition alone in melanoma”, *N Engl J Med* 371.20 (2014), pp. 1877–1888.

[14] H. Rizos, A. M. Menzies, G. M. Pupo, M. S. Carlino, C. Fung, J. Hyman, et al. “BRAF inhibitor resistance mechanisms in metastatic melanoma: spectrum and clinical impact”, *Clin Cancer Res* 20.7 (2014), pp. 1965–1977.

[15] P. Queirolo and F. Spagnolo. “BRAF plus MEK-targeted drugs: a new standard of treatment for BRAF-mutant advanced melanoma”, *Cancer Metastasis Rev* 36.1 (2017), pp. 35–42.

[16] P. A. Ascierto, R. Dummer, H. J. Gogas, K. T. Flaherty, A. Arance, M. Mandala, et al. “Update on tolerability and overall survival in COLUMBUS: landmark analysis of a randomised phase 3 trial of encorafenib plus binimetinib vs vemurafenib or encorafenib in patients with BRAF V600-mutant melanoma”, *Eur J Cancer* 126 (2020), pp. 33–44.

[17] C. Y. Huang and J. E. Ferrell. “Ultrasensitivity in the mitogen-activated protein kinase cascade”, *Proc Natl Acad Sci USA* 93.19 (1996), pp. 10078–10083.

[18] W. S. VanScyoc, G. A. Holdgate, J. E. Sullivan, and W. H. Ward. “Enzyme kinetics and binding studies on inhibitors of MEK protein kinase”, *Biochemistry* 47.17 (2008), pp. 5017–5027.

[19] S. J. Mansour, J. M. Candia, J. E. Matsuura, M. C. Manning, and N. G. Ahn. “Interdependent domains controlling the enzymatic activity of mitogen-activated protein kinase kinase 1”, *Biochemistry* 35.48 (1996), pp. 15529–15536.

[20] FDA (US Food and Drug Administration). “Reference ID: 4255750”, *Available on: https://www.accessdata.fda.gov/drugsatfda_docs/label/2018/202806s008lbl.pdf* (2018).

[21] A. G. Gilmartin, M. R. Bleam, A. Groy, K. G. Moss, E. A. Minthorn, S. G. Kulkarni, et al. “GSK1120212 (JTP-74057) is an inhibitor of MEK activity and activation with favorable pharmacokinetic properties for sustained in vivo pathway inhibition”, *Clin Cancer Res* 17.5 (2011), pp. 989–1000.

[22] A. J. King, M. R. Arnone, M. R. Bleam, K. G. Moss, J. Yang, K. E. Fedorowicz, et al. “Dabrafenib; preclinical characterization, increased efficacy when combined with trametinib, while BRAF/MEK tool combination reduced skin lesions”, *PLoS One* 8.7 (2013), e67583.

[23] R. Roskoski. “Allosteric MEK1/2 inhibitors including cobimetanib and trametinib in the treatment of cutaneous melanomas”, *Pharmacol Res* 117 (2017), pp. 20–31.

[24] G. Hatzivassiliou, K. Song, I. Yen, B. J. Brandhuber, D. J. Anderson, R. Alvarado, et al. “RAF inhibitors prime wild-type RAF to activate the MAPK pathway and enhance growth”, *Nature* 464.7287 (2010), pp. 431–435.

[25] T. R. Rheault, J. C. Stellwagen, G. M. Adjabeng, K. R. Hornberger, K. G. Petrov, A. G. Waterson, et al. “Discovery of Dabrafenib: A Selective Inhibitor of Raf Kinases with Anti-tumor Activity against B-Raf-Driven Tumors”, *ACS Med Chem Lett* 4.3 (2013), pp. 358–362.

[26] J. Tsai, J. T. Lee, W. Wang, J. Zhang, H. Cho, S. Mamo, et al. “Discovery of a selective inhibitor of oncogenic B-Raf kinase with potent antimelanoma activity”, *Proc Natl Acad Sci U S A* 105.8 (2008), pp. 3041–3046.

[27] P. Koelblinger, O. Thuerigen, and R. Dummer. “Development of encorafenib for BRAF-mutated advanced melanoma”, *Curr Opin Oncol* 30.2 (2018), pp. 125–133.

[28] T. Yamamoto, M. Ebisuya, F. Ashida, K. Okamoto, S. Yonehara, and E. Nishida. “Continuous ERK activation downregulates antiproliferative genes throughout G1 phase to allow cell-cycle progression”, *Curr Biol* 16.12 (2006), pp. 1171–1182.

[29] J. C. Chambard, R. Lefloch, J. Pouysségur, and P. Lenormand. “ERK implication in cell cycle regulation”, *Biochim Biophys Acta* 1773.8 (2007), pp. 1299–1310.

[30] R. J. Tallarida. “Quantitative methods for assessing drug synergism”, *Genes Cancer* 2.11 (2011), pp. 1003–1008.

[31] W. R. Burack and T. W. Sturgill. “The activating dual phosphorylation of MAPK by MEK is nonprocessive”, *Biochemistry* 36.20 (1997), pp. 5929–5933.

[32] J. E. Ferrell and R. R. Bhatt. “Mechanistic studies of the dual phosphorylation of mitogen-activated protein kinase”, *J Biol Chem* 272.30 (1997), pp. 19008–19016.

[33] N. I. Markevich, J. B. Hoek, and B. N. Kholodenko. “Signaling switches and bistability arising from multisite phosphorylation in protein kinase cascades”, *J Cell Biol* 164.3 (2004), pp. 353–359.

[34] J. E. Ferrell and E. M. Machleder. “The biochemical basis of an all-or-none cell fate switch in Xenopus oocytes”, *Science* 280.5365 (1998), pp. 895–898.

[35] F. A. Brightman and D. A. Fell. “Differential feedback regulation of the MAPK cascade underlies the quantitative differences in EGF and NGF signalling in PC12 cells”, *FEBS Lett* 482.3 (2000), pp. 169–174.

[36] B. Schoeberl, C. Eichler-Jonsson, E. D. Gilles, and G. Müller. “Computational modeling of the dynamics of the MAP kinase cascade activated by surface and internalized EGF receptors”, *Nat Biotechnol* 20.4 (2002), pp. 370–375.

[37] G. S. Falchook, G. V. Long, R. Kurzrock, K. B. Kim, H. T. Arkenau, M. P. Brown, et al. “Dose selection, pharmacokinetics, and pharmacodynamics of BRAF inhibitor dabrafenib (GSK2118436)”, *Clin Cancer Res* 20.17 (2014), pp. 4449–4458.

[38] K. A. Rejniak and A. R. Anderson. “Hybrid models of tumor growth”, *Wiley Interdiscip Rev Syst Biol Med* 3.1 (2011), pp. 115–125.

[39] R. C. Rockne, A. Hawkins-Daarud, K. R. Swanson, J. P. Sluka, J. A. Glazier, P. Macklin, et al. “The 2019 mathematical oncology roadmap”, *Phys Biol* 16.4 (2019), p. 041005.

[40] Y. Mebratu and Y. Tesfaigzi. “How ERK1/2 activation controls cell proliferation and cell death: Is subcellular localization the answer?”, *Cell Cycle* 8.8 (2009), pp. 1168–1175.

[41] S. Hamis, P. Nithiarasu, and G. G. Powathil. “What does not kill a tumour may make it stronger: In silico insights into chemotherapeutic drug resistance”, *J Theor Biol* 454 (2018), pp. 253–267.

[42] S. Hamis, M. Kohandel, L. J. Dubois, A. Yaromina, P. Lambin, and G. G. Powathil. “Combining hypoxia-activated prodrugs and radiotherapy in silico: Impact of treatment scheduling and the intra-tumoural oxygen landscape”, *PLoS Comput Biol* 16.8 (2020), e1008041.

[43] S. Hamis, G. G. Powathil, and M. A. J. Chaplain. “Blackboard to Bedside: A Mathematical Modeling Bottom-Up Approach Toward Personalized Cancer Treatments”, *JCO Clin Cancer Inform* 3 (2019), pp. 1–11.

[44] I. Smalley, E. Kim, J. Li, P. Spence, C. J. Wyatt, Z. Eroglu, et al. “Leveraging transcriptional dynamics to improve BRAF inhibitor responses in melanoma”, *EBioMedicine* 48 (2019), pp. 178–190.